ELSEVIER

Tectonophysics 350 (2002) 255–271

TECTONOPHYSICS

www.elsevier.com/locate/tecto

Geochronological constraints on Paleoarchean thrust-nappe and Neoarchean accretionary tectonics in southern West Greenland

Simon Hanmer[a,*], Michael A. Hamilton[a], James L. Crowley[b,1]

[a]*Continental Geoscience Division, Geological Survey of Canada, 601 Booth Street, Ottawa, ON, Canada K1A 0E8*
[b]*Department of Earth Sciences, Memorial University of Newfoundland, St. John's, NF, Canada A1B 3X5*

Received 6 June 2001; accepted 15 February 2002

Abstract

Major regional deformation and metamorphic events in the Godthåbsfjord region, southern West Greenland, occurred at ~3650 and 2820–2720 Ma (e.g. Precambrian Res. 78 (1996) 1). New geochronological constraints (U–Pb zircon, Sensitive High Resolution Ion Microprobe [SHRIMP] and thermal ionisation mass spectrometry [TIMS]) have been obtained from a stack of mylonitic, crystalline thrust-nappes in the footwall of the western part of the Paleoarchean (~3.8–3.7 Ga) Isua Greenstone Belt, Isukasia. A mylonitic tonalite sheet, interpreted to have intruded synkinematically with respect to mylonitisation, yields a magmatic crystallisation age of 3640 ± 3 Ma. A cross-cutting pegmatite and a post-kinematic tonalite pluton yield magmatic crystallisation ages of 2948 ± 8 and 2991 ± 2 Ma, respectively. Accordingly, we interpret the thrust-nappe stack to have formed during the Paleoarchean (~3640 Ma), making it the oldest example known on Earth. The similarity of this structural regime to that of modern mountain belts suggests that Paleoarchean and modern continental crust were comparable in terms of mechanical strength and constitution. Southern West Greenland has been interpreted in terms of Neoarchean accretion, comparable with modern plate tectonics (e.g. Earth Planet. Sci. Lett. 142 (1996) 353). Isukasia lies just east of a purported Neoarchean accretionary boundary between the Akia terrane to the Northwest and the Akulleq terrane to the Southeast. The Akia terrane was previously considered to overthrust the Akulleq terrane at ~2820–2720 Ma. Our geochronological and geological data indicate (i) that the two "terranes", as presently defined, were stitched at 2991 ± 2 Ma and (ii) that thrusting across the boundary was directed toward the Akia terrane. Therefore, we suggest that the Akia–Akulleq interface was not a fundamental tectonic structure during the Neoarchean, and we question its identification as an accretionary boundary. © 2002 Elsevier Science B.V. All rights reserved.

Keywords: Isua; Greenland; Paleoarchean thrust-nappes; Neoarchean tectonics

1. Introduction

The extrapolation of actualistic plate tectonic paradigms to the Archean continues to be the subject of vigorous debate (e.g. Hamilton, 1998; de Wit, 1998). In the Godthåbsfjord region of southern West Green-

* Corresponding author. Fax: +1-613-943-5318.
E-mail addresses: shanmer@nrcan.gc.ca (S. Hanmer), hamilton@nrcan.gc.ca (M.A. Hamilton), jcrowley@sparky2.esd.mun.ca (J.L. Crowley).
[1] Present address: Department of Earth, Atmospheric and Planetary Sciences, MIT, Cambridge, MA 02139, USA.

0040-1951/02/$ - see front matter
PII: S0040-1951(02)00120-8

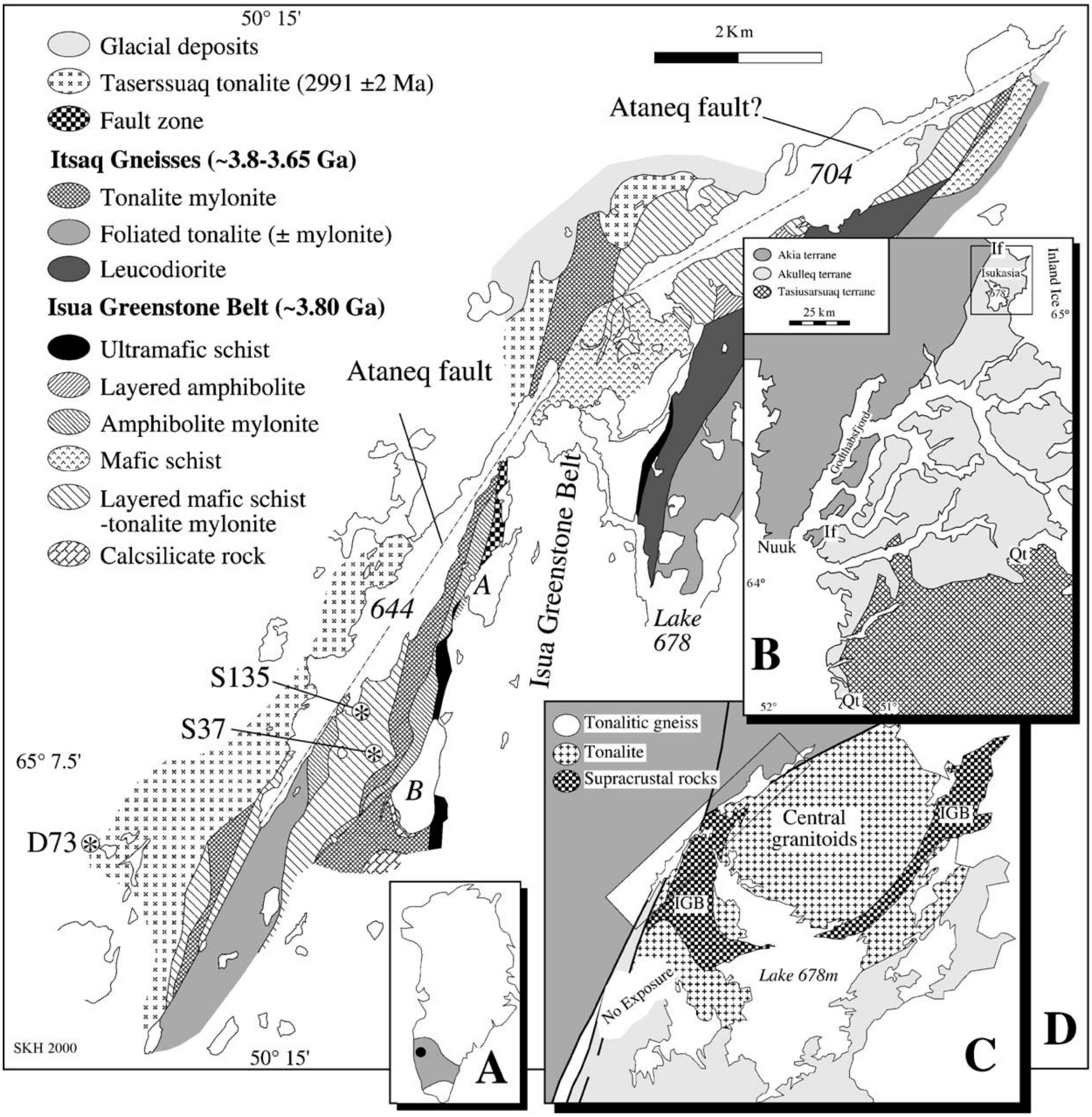

Fig. 1. Geological sketch map of northwest termination of the western Isua Greenstone Belt, Isukasia (D; after Hanmer and Greene, in press). Location in southern West Greenland and relative to the Isua Greenstone Belt (IGB) are indicated by the tiled insets (A, B, C). Rectangular box in C is location of geology of D. Numbered asterisks are locations of geochronology samples.

land (Fig. 1A and B), a Neoarchean[2] history of terrane accretion has been identified and tentatively interpreted in terms of ~2820–2720 Ma convergent margins and continental collision, similar to tectonic processes that operated in younger orogenic belts (Friend et al., 1988, 1996; Nutman et al., 1989; McGregor et al., 1991; Friend and Nutman, 2001). In a more recent interpretation, the assembled Archean

[2] Archean era as in Okulitch, 1999.

terranes are no longer associated with continental collision. Rather, they are interpreted as blocks of older crust accreted to the remnants of several ~2730–2700 Ma arcs of unknown polarity that make up the northern and western parts of the Greenland craton (Friend et al., 1996). According to this model, an Akulleq terrane was first overthrust by a Tasiusarsuaq terrane on its southern flank, then by an Akia terrane on its northern margin (Fig. 1B).

The Isua Greenstone Belt, Isukasia, is located immediately east of the northern part of the Akia–Akulleq boundary (Fig. 1B and C). Nutman (1986) identified the northern limit of intense Neoarchean regional deformation and metamorphism within the Akulleq terrane, south of the Isua Greenstone Belt (Fig. 1C; ~2820–2720 Ma, Nutman et al., 1996; Friend et al., 1996). In later publications (Nutman et al., 1999, Fig. 1), this limit was extended to the Northwest, apparently placing the rocks immediately west of the Isua Greenstone Belt within the domain of Neoarchean tectonothermal reworking. However, our detailed structural field mapping indicates that the principal deformation there is related to southwest- and northwest-directed thrusting events that appear to have occurred prior to ~3000 Ma (Hanmer and Greene, 2002).

In this contribution, we present U–Pb zircon data that provide new age constraints on deformation along the Isukasia segment of the Akia–Akulleq boundary. We propose that (i) polyphase thrust-nappe tectonics on the Akulleq side of the boundary occurred at ~3640 Ma and that the boundary was stitched by a ~3000-Ma pluton, and (ii) the relationship of the boundary to purported Neoarchean accretionary tectonics should be reconsidered.

2. Neoarchean terrane accretion

Previous workers have identified terrane accretion in the Godthåbsfjord region on the basis of contrasting geological histories in different parts of what was previously considered to be a single terrane (Fig. 1B; McGregor et al., 1991; Friend et al., 1996 and detailed references therein). The following summary draws principally on their work, unless otherwise indicated.

The Akulleq terrane is predominantly composed of Paleoarchean to Mesoarchean >3800–3600 Ma granitoid and supracrustal rocks of the Itsaq Gneiss Complex that locally experienced granulite facies metamorphism at ~3650 Ma (Nutman et al., 1996; Crowley and Myers, 2001), and Neoarchean supracrustal rocks intruded by the granitoid precursors of the ~2820-Ma Ikkatoq gneisses. The Akia terrane mostly comprises Mesoarchean (~3220–3000 Ma) dioritic, tonalitic, and granitic gneisses, affected in its central parts by a regional granulite facies event at ~3000 Ma (see also Garde et al., 2000). A Sm–Nd "errorchron" for the central part of the Akia terrane suggests extraction from a mildly depleted mantle source at ~3050 Ma, which contrasts with a similarly determined extraction age of ~3675 Ma for the Akulleq terrane (Garde et al., 2000). The Tasiusarsuaq terrane is principally composed of Neoarchean ~2920–2800 Ma tonalitic gneisses and older supracrustal rocks that recorded granulite facies metamorphism at ~2810 Ma.

The terrane boundaries in the Godthåbsfjord region (Fig. 1B) are marked by narrow, amphibolite facies mylonite zones, up to 50 m thick. The Tasiusarsuaq terrane is underlain by the Qarliit nunaat shear zone, which was interpreted as a thrust because it emplaces granulite facies rocks over amphibolite facies rocks, and was correlated with geometrically compatible fold nappe development in the Akulleq footwall (Friend et al., 1996). The Akia terrane is bounded to the Southeast by the Ivinnguit fault, a structure that is reworked by narrow (10–100 m), Proterozoic, greenschist facies, mylonitic, and cataclastic zones (Smith and Dymek, 1983; Friend and Nutman, 1991). It was interpreted as a thrust because (i) locally, where it is not affected by younger structures, it dips moderately to the Northwest and carries an extension lineation that pitches moderately to the west, and (ii) it places the predominantly granulite facies Akia terrane over the lower grade components of the Akulleq terrane (Friend et al., 1996). The Qarliit nunaat shear zone is deformed by upright folds that decrease in amplitude with distance away from it and do not deform the Ivinnguit fault. Accordingly, accretion of the Tasiusarsuaq terrane was thought to have occurred prior to that of the Akia terrane (Friend et al., 1996).

Timing of accretion was determined according to two principal criteria (Friend et al., 1996). The maximum age of terrane assembly was interpreted from the age of the youngest rocks cut by mylonites at the boundaries; the ~2820-Ma magmatic age of the Ikkatoq gneisses of the Akulleq terrane and the contemporaneous granulite facies gneisses of the Tasiusarsuaq terrane. The minimum age was interpreted from the first event common to all of the juxtaposed terranes, granitoid sheets dated at ~2720 Ma. In the Akulleq terrane, these are associated with an important anatectic event, whereas in the other two terranes they form simple intrusive sheets (for details of the Neoarchean accretionary model, see McGregor et al., 1991; Friend et al., 1996).

3. Isukasia

The Isukasia area, at the western edge of the Akulleq terrane, adjacent to the Inland Ice, contains the supracrustal rocks of the Paleoarchean (~3800–3700 Ma; Nutman et al., 1997, 2001a; Frei and Rosing, 2001) Isua Greenstone Belt (Fig. 1C; e.g. Nutman, 1984, 1986; Appel et al., 1998a,b and references therein). The arcuate supracrustal belt is flanked to the north and south by variably deformed, metamorphosed tonalitic, dioritic, and granitic plutonic rocks of the >3800–3600-Ma Itsaq Gneiss Complex (Nutman et al., 1993, 1996, 1999 and references therein; Crowley and Myers, 2001). However, there is some debate as to whether the granitoids crystallised magmatically at ~3650 Ma and contain abundant inherited zircon (e.g. Kamber and Moorbath, 1998; Whitehouse et al., 1999; Nutman et al., 2000 and references therein).

Until very recently, few structural studies have been undertaken in the Isua Greenstone Belt and the flanking metagranitoids (James, 1976; see also Myers, 2001a,b). Foliations in the greenstone belt and the Itsaq Gneiss Complex are cross-cut by the Tarssartôq mafic dyke swarm that has yielded ~3500 Ma magmatic crystallisation ages and is correlated with the Ameralik dykes of the Godthåbsfjord area (U–Pb zircon Sensitive High Resolution Ion Microprobe (SHRIMP); Nutman et al., 1996, 1997, 2001b; White et al., 2000). The dykes are particularly common in the central gneisses north of the supracrustal rocks (Fig. 1C). The oldest preserved metamorphism in the Isua Greenstone Belt occurred at ~3750–3700 Ma (Pb–Pb, Sm–Nd, and Lu–Hf ages, Frei et al., 1999; Blichert-Toft and Frei, 2001; see also Moorbath et al., 1973), followed by a major tectonothermal and plutonic event at ~3650 Ma (Nutman et al., 1996; Kamber and Moorbath, 1998). Boak and Dymek (1982), Hayashi et al. (2000), and Rollinson (2000) have independently obtained ~550 °C at ~5 kbar from garnet–biotite–staurolite and muscovite–biotite–kyanite metamorphic assemblages, presumably related to the ~3650 Ma event.

3.1. Thrust-nappe stack

In the Isukasia area, the poorly known northern segment of the Ivinnguit fault is spatially coincident with the Proterozoic Ataneq fault over much of its strike length (Fig. 1D; e.g. Friend and Nutman, 1991). Field mapping in the footwall immediately beneath the western limb of the arcuate Isua Greenstone Belt has documented a stack of amphibolite facies, mylonitic, crystalline thrust-nappes that straddle and are cut by the narrow (~10 m) chlorite–sericite mylonites of the Ataneq fault (Fig. 1D; Hanmer and Greene, 2002). The thrust-nappe stack comprises panels of tonalitic and amphibolitic mylonite and mafic schist, all dipping moderately beneath the western part of the greenstone belt. Crystalline thrust-nappes, whose internal structure comprises a multilayer of mylonitic tonalite sheets and mafic schist, are penetratively affected by intrafolial sheath folds that deform the layer-parallel mylonitic foliation. Kinematic analysis of the widely developed and abundant sheath folds reveals a three-part displacement history within the thrust-nappe stack: initial, top-to-southwest longitudinal thrusting, followed by top-to-northwest transverse thrusting, and subsequent top-to-southeast extensional collapse of the thickened crust. If this polyphase structural sequence is related to a common orogenic event, it resembles a tectonic style characteristic of Phanerozoic and modern mountain belts (see Hanmer and Greene, 2002 for detailed discussion). However, in the context of the Neoarchean accretionary tectonic model for southern West Greenland, the kinematics of the thrust-nappe stack are incompatible with the tectonic emplacement of the Akia terrane to the east and south over the Akulleq terrane.

The multilayered panels of the mylonitic thrust-nappe stack are the product of synkinematic injection of thin (1–10 m), grey and white tonalite sheets into a strongly foliated amphibole–chlorite mafic schist

(Hanmer and Greene, 2002). Both grey and white tonalites are pervasively mylonitised with well-developed ribbon fabrics. However, in detail, less strongly deformed white tonalite sheets locally cut grey tonalitic mylonite, but are themselves subsequently mylonitised. From this, we deduce that the white mylonitic tonalite sheets at least were injected synkinematically with respect to mylonitisation. Two intrusive sheets were sampled for SHRIMP analysis (see Fig. 1D for locations). The first sample (S135) is a homogeneous, fine-grained, annealed, white tonalite mylonite, approximately 1 m thick, that outlines the topology of a sheath fold, 5 m in maximum wavelength, that developed during top-to-northwest thrusting (Fig. 2). The tonalite sheet is concordant with the mylonite foliation in the rest of the multilayer that is deformed by the sheath fold. Accordingly, it could be conservatively interpreted as providing a maximum age for mylonitisation. However, because it appears to belong to the swarm of synkinematic tonalite sheets, we will interpret its magmatic crystallisation age as indicative of the time of mylonitisation. The second sample (S37) is a clean pegmatite that cross-cuts a mylonitic multilayer at a high angle, near the base of a ~100-m-thick stack of sheath folds that developed during top-to-southwest thrusting (Fig. 3). Although the pegmatite is non-foliated, it has been deformed into open folds. We interpret S37 to be a late pegmatite, emplaced after shearing and mylonitisation, that will provide a minimum age for intense deformation of the thrust-nappe stack. The open folding of the pegmatite represents a late deformation pulse that resulted in moderate tightening of the earlier formed intrafolial sheath folds.

Fig. 2. Sample site for S135. The sample was taken (white circle) from a concordant tonalite mylonite layer in mafic schist–tonalite mylonite. The layer is deformed about a sheath fold. The sheath fold axis is parallel to the line of sight at A and A′. Hammer for scale approximately midway between A and A′.

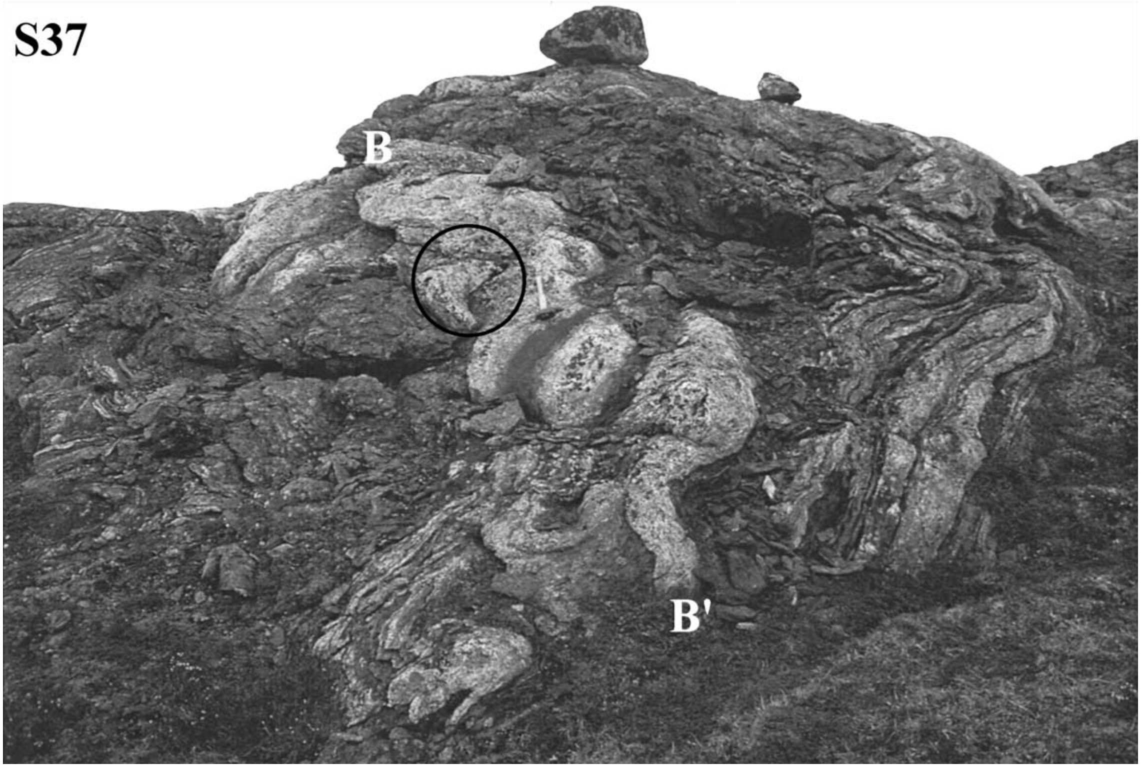

Fig. 3. Non-foliated, mildly folded pegmatite, B to B′, cuts mafic schist–tonalite mylonite at a high angle. Sheath folds of the mylonite fabric and layering, cut by the pegmatite, are not visible in this photo.

3.2. Taserssuaq tonalite: a stitching pluton

Mylonites of the crystalline thrust-nappe stack are intruded by the Taserssuaq tonalite (Fig. 1D; Hanmer and Greene, 2002), a batholithic body that occupies the eastern third of the Akia terrane (e.g. Garde, 1987; Garde, 1997). It is a largely homogeneous body with some dioritic components extending from the Inland Ice to the Godthåbsfjord area, where it has a similar intrusive relationship with rock units on its eastern margin (Chadwick et al., 1983). In the Isukasia area, the Taserssuaq tonalite is an equigranular, medium-grained (~ 5 mm), leucocratic tonalite with a weakly developed shape fabric marked by aligned biotite. Because the quartz grains are unstrained, we interpret this to be a magmatic foliation. At its eastern margin, the tonalite contains grey leucodioritic inclusions. Near the contact, the tonalite is charged with misoriented inclusions of foliated leucocratic dioritic gneiss with more melanocratic bands, intruded by tonalite veins that cut the gneissic layering. We interpret the dioritic marginal phase as cogenetic with the tonalite. Several rafts, 50 m long by 10 m thick, of openly folded, layered mylonite are entirely included and misoriented within the tonalite, demonstrating that the Taserssuaq tonalite was emplaced at least post-mylonitisation and likely after deformation of the mylonite and its intrafolial sheath folds by late, upright, horizontal folding (see Hanmer and Greene, 2002).

Although the thrust-nappe stack is cut by the Proterozoic Ataneq fault, the nature and tectonometamorphic history of the mylonitic crystalline thrust-nappes are the same on either side of the fault (Fig. 1D; Hanmer and Greene, 2002). Therefore, the tonalite stitches the Akia and Akulleq terranes, as they are presently defined. The Taserssuaq tonalite has previously been dated at 2982$\pm$7 Ma (Garde et al., 1986; Garde, 1997), suggesting that the thrust-nappe stack formed prior to the 2820–2720-Ma Neoarchean deformation events. However, the sample dated by Garde et al. (1986) comes from a site ~25 km west of the observed intrusive relationship, and the possibility that the Taserssuaq tonalite contains Neoarchean phases has not been eliminated. Accordingly, a sample (D73) was taken within the clean tonalite, ~1 km west of the mylonites (D73; Fig. 3), in order to avoid possible contamination by dioritic inclusions.

4. Geochronology

Zircon populations in the early Archean gneisses of southern West Greenland are notoriously complex but are amenable to ion microprobe analysis supported by cathodoluminescence (CL) imaging (e.g. Whitehouse et al., 1999; Nutman et al., 2000 and references therein). Samples S135 and S37 were analysed using the Sensitive High Resolution Ion Microprobe (SHRIMP II) facility at the Geological Survey of Canada (GSC), whereas the Taserssuaq tonalite (D73) was dated by thermal ionisation mass spectrometry (TIMS) in the Geochronology Laboratory at Memorial University.

4.1. SHRIMP

Detailed analytical and data reduction procedures for the SHRIMP have been described in detail by Stern (1997). Zircons from each sample were arranged along with fragments of the GSC laboratory zircon reference standard (BR266 zircon; $^{206}Pb/^{238}U$ isotope dilution age=559 Ma), cast in epoxy grain mounts, and polished with diamond compound to reveal the grain centres. The grains were then imaged with a Cambridge Instruments scanning electron microscope (SEM) equipped with cathodoluminescence (CL) and backscatter detectors in order to identify compositional zoning and fracturing and to guide ion probe spot site selection. Data were acquired using a mass-filtered O^- primary beam with approximate sputtering diameters of 29×35 and 10×13 μm, carried out over two separate sessions. Primary beam currents averaged approximately 15.0 and 2.5 nA using the larger and smaller O^- beam apertures, respectively, and mass resolution ranged between 5450 and 5750. Correction of the measured isotopic ratios for common Pb was estimated from monitored ^{204}Pb, and the corrected ratios and ages are reported with 1σ analytical errors (68% confidence; Table 1). Calculated age intercepts and weighted mean ages, however, are presented in the text at 95% confidence levels.

Ion microprobe U–Th–Pb analytical data for zircons from the samples are presented in Table 1 and in concordia plots in Fig. 4. We follow the approach of other recent workers dealing with in situ analysis of zircon grains in making extensive use of cathodoluminescence and backscattered electron imaging of grains as a necessary prerequisite before ion probe analysis (e.g. Whitehouse et al., 1999; Nutman et al., 1999). We regard this as the most useful method of obtaining unambiguous ages on zircons, which routinely show internal structural complexities on the scale of a few microns to a few tens of microns. In this study, because of the variable thicknesses of individual growth structures from grain to grain, it was rarely possible to analyse every domain (core, mantle or rim) within each crystal. Commonly, it was more practical to obtain core and mantle ages from one grain and an overgrowth from another, or some other combination. Nonetheless, a coherent picture of the growth systematics became apparent through careful documentation of the SEM textures coupled with the ion probe results.

4.1.1. Tonalite mylonite, S135

Zircons recovered from the tonalite mylonite were chosen from the two least paramagnetic fractions at maximum current and 1° side slope on a Frantz™ isodynamic separator. These range in size mostly between 50 and 150 μm, though some grains are larger (up to 250 μm). Zircons from this sample show a variety of morphological characteristics: colour ranges from nearly colourless to pale brown and reddish brown, prismatic forms dominate with length/width ratios of 2:1 to 3:1, terminations are rarely sharp, and some grains are completely anhedral, while others are subequant and multifaceted. Transmitted light microscopy shows that many grains exhibit internal oscillatory zoning and, in some cases, distinct rounded or irregular cores.

Backscattered electron (BSE) and CL imaging, when combined with observations from transmitted light microscopy, allow a ready characterisation of the internal structural complexities of the grains (Fig. 5a). Under CL, most zircons within the tonalite mylon-

Table 1
Ion microprobe (SHRIMP II) U–Th–Pb data for zircons from syn-kinematic tonalite (S135) and deformed pegmatite (S37), from the Isukasia region, southern West Greenland

Spot	Structure	[U] (ppm)	[Th] (ppm)	Th/U	[Pb*] (ppm)	^{204}Pb (ppb)	f206c (%)	^{206}Pb/^{238}U	±1σ	^{207}Pb/^{235}U	±1σ	^{207}Pb/^{206}Pb	±1σ	Age (Ma)‡	±1σ	Conc. (%)
S135, tonalite mylonite																
14.1	core¶	160	110	0.71	164	67	1.07	0.7770	0.0067	38.064	0.338	0.3553	0.0005	3729.8	2.2	99.4
22.2	core§	241	204	0.87	239	2	0.02	0.7263	0.0123	34.765	0.599	0.3472	0.0007	3694.5	3.0	95.3
10.1	core¶	126	113	0.93	130	1	0.02	0.7590	0.0071	35.294	0.340	0.3373	0.0005	3650.4	2.3	99.7
4.1	core¶	100	98	1.01	104	3	0.08	0.7550	0.0073	35.026	0.358	0.3365	0.0008	3646.8	3.8	99.4
3.1	core¶	205	157	0.79	206	2	0.02	0.7572	0.0061	35.068	0.292	0.3359	0.0005	3644.2	2.0	99.7
27.2	core≈	117	106	0.93	121	3	0.07	0.7592	0.0062	35.159	0.295	0.3359	0.0004	3644.1	1.7	99.9
13.1	core§	111	75	0.70	109	1	0.03	0.7495	0.0064	34.709	0.317	0.3359	0.0008	3644.0	3.7	98.9
6.1	core¶	114	101	0.92	113	2	0.05	0.7315	0.0061	33.872	0.309	0.3358	0.0009	3644.0	4.3	97.1
8.1	core≈	220	174	0.82	218	5	0.06	0.7418	0.0061	34.327	0.291	0.3356	0.0004	3643.0	2.0	98.2
11.1	core≈	91	79	0.89	91	1	0.03	0.7432	0.0063	34.381	0.308	0.3355	0.0007	3642.5	3.3	98.4
19.2	core§	811	107	0.14	738	4	0.01	0.7715	0.0066	35.684	0.329	0.3355	0.0009	3642.3	4.1	101.2
29.2	Mantle†	416	106	0.26	374	4	0.03	0.7441	0.0120	34.406	0.576	0.3354	0.0010	3641.7	4.3	98.5
17.2	mantle§	718	148	0.21	653	5	0.02	0.7603	0.0173	35.125	1.030	0.3351	0.0053	3640.5	24.4	100.1
21.2	core≈	99	91	0.95	102	10	0.27	0.7543	0.0073	34.835	0.359	0.3349	0.0008	3639.9	3.8	99.5
24.1	core†	238	183	0.79	230	2	0.02	0.7287	0.0119	33.620	0.604	0.3346	0.0019	3638.4	8.8	97.0
31.1	core≈	334	324	1.00	353	3	0.02	0.7703	0.0065	35.523	0.307	0.3345	0.0003	3637.7	1.5	101.2
9.1	core†	147	113	0.79	149	<1	0.00	0.7624	0.0065	35.148	0.326	0.3344	0.0009	3637.3	4.0	100.4
7.1	core¶	213	156	0.76	212	2	0.02	0.7534	0.0064	34.690	0.308	0.3340	0.0006	3635.3	2.8	99.6
16.1	core†	169	114	0.70	161	11	0.18	0.7263	0.0066	33.399	0.321	0.3335	0.0007	3633.4	3.1	96.9
15.1	core?†	158	163	1.06	161	17	0.30	0.7352	0.0073	33.804	0.359	0.3335	0.0009	3633.1	4.2	97.8
5.1	core?†	154	128	0.86	154	<1	0.00	0.7475	0.0068	34.351	0.340	0.3333	0.0009	3632.4	4.3	99.1
1.1	core§	1024	157	0.16	921	7	0.02	0.7613	0.0061	34.945	0.290	0.3329	0.0004	3630.6	2.0	100.5
23.1	mantle?§	600	133	0.23	529	4	0.02	0.7346	0.0119	33.591	0.551	0.3316	0.0005	3624.6	2.1	98.0
12.1	core?†	170	134	0.81	168	2	0.04	0.7454	0.0067	34.062	0.319	0.3314	0.0006	3623.8	3.0	99.1
18.1	core§	1313	123	0.10	1164	9	0.02	0.7606	0.0123	34.607	0.573	0.3300	0.0006	3617.0	2.9	100.8
2.2	core§	178	212	1.23	189	26	0.39	0.7430	0.0067	33.696	0.317	0.3289	0.0006	3612.1	2.7	99.2
29.1	core§	874	65	0.08	740	112	0.35	0.7341	0.0119	32.729	0.808	0.3234	0.0054	3585.9	26.0	99.0
26.1	mantle†	609	88	0.15	520	9	0.04	0.7307	0.0122	32.394	0.575	0.3215	0.0014	3577.1	6.5	98.9
25.1	core≈	1124	66	0.06	888	72	0.19	0.6927	0.0116	29.657	0.509	0.3105	0.0006	3523.5	3.1	96.3
17.1	core≈	1262	66	0.05	992	8	0.02	0.6957	0.0179	28.572	0.989	0.2979	0.0060	3459.1	31.6	98.4
28.1	core≈	2955	181	0.06	1828	32	0.04	0.5753	0.0093	18.456	0.301	0.2327	0.0003	3070.4	2.0	95.4
2.1	rim§	482	8	0.02	294	5	0.03	0.5797	0.0047	17.556	0.146	0.2197	0.0002	2978.2	1.7	99.0
17.3	rim§	749	42	0.06	451	483	2.24	0.5689	0.0107	16.843	0.350	0.2147	0.0015	2941.6	11.4	98.7
19.1	rim§	458	36	0.08	267	661	5.04	0.5499	0.0095	16.127	0.403	0.2127	0.0034	2926.3	26.1	96.5
27.1	rim§	218	4	0.02	126	4	0.06	0.5513	0.0094	16.078	0.286	0.2115	0.0008	2917.2	5.7	97.0
8.2	rim§	247	6	0.03	138	16	0.24	0.5392	0.0093	14.861	0.276	0.1999	0.0010	2825.2	8.2	98.4
22.1	mantle†	2450	178	0.08	1431	2	0.00	0.5587	0.0090	15.038	0.248	0.1952	0.0004	2786.8	3.7	102.7
20.1	rim§	580	38	0.07	317	14	0.09	0.5255	0.0085	13.784	0.243	0.1903	0.0010	2744.3	8.5	99.2
21.1	rim§	751	15	0.02	376	822	4.20	0.5041	0.0083	12.159	0.227	0.1749	0.0012	2605.3	11.8	101.0
S37, pegmatite																
3.2	core§	252	106	0.43	226	2	0.02	0.7198	0.0126	33.390	0.626	0.3364	0.0017	3646.6	7.7	95.9
17.1	core≈	516	401	0.80	509	18	0.10	0.7409	0.0122	34.216	0.575	0.3349	0.0007	3639.8	3.3	98.2
1.1	core†	305	81	0.27	270	2	0.02	0.7343	0.0063	33.637	0.294	0.3322	0.0003	3627.5	1.4	97.8
19.1	core≈	151	30	0.21	128	1	0.02	0.7124	0.0124	32.529	0.589	0.3312	0.0010	3622.4	4.7	95.7
13.1	core≈	301	228	0.78	290	3	0.03	0.7240	0.0128	33.034	0.628	0.3309	0.0017	3621.3	7.8	97.0
17.2	inner mantle†	730	67	0.09	630	23	0.09	0.7401	0.0121	33.713	0.563	0.3304	0.0007	3618.9	3.3	98.7
20.1	core≈	421	262	0.64	399	6	0.04	0.7357	0.0121	33.254	0.562	0.3278	0.0008	3606.9	3.9	98.6
3.1	inner mantle§	546	85	0.16	475	10	0.05	0.7373	0.0060	33.298	0.274	0.3275	0.0002	3605.6	1.1	98.8
15.1	core≈	936	42	0.05	807	6	0.02	0.7504	0.0128	33.636	0.610	0.3251	0.0015	3594.2	7.0	100.4

Table 1 (*continued*)

Spot	Structure	[U] (ppm)	[Th] (ppm)	Th/U	[Pb*] (ppm)	^{204}Pb (ppb)	f206c (%)	^{206}Pb/^{238}U	±1σ	^{207}Pb/^{235}U	±1σ	^{207}Pb/^{206}Pb	±1σ	Age (Ma)‡	±1σ	Conc. (%)
S37, pegmatite																
6.1	core§	139	59	0.44	126	4	0.07	0.7345	0.0064	32.361	0.291	0.3196	0.0004	3567.7	1.9	99.5
1.3	core†	394	85	0.22	337	5	0.04	0.7222	0.0117	31.749	0.527	0.3188	0.0007	3564.2	3.4	98.3
1.2	mantle†	246	29	0.12	199	1	0.01	0.6953	0.0118	30.271	0.542	0.3158	0.0013	3549.4	6.2	95.9
18.1	core ≈	992	22	0.02	800	185	0.53	0.7141	0.0117	30.617	0.602	0.3110	0.0028	3525.8	14.0	98.5
9.1	core§	957	33	0.04	762	37	0.11	0.7029	0.0057	29.953	0.247	0.3091	0.0003	3516.2	1.4	97.6
2.1	mantle§	1570	99	0.07	980	3	0.01	0.5878	0.0047	17.639	0.143	0.2176	0.0001	2963.2	0.7	100.6
7.1	core§	615	111	0.19	395	2	0.01	0.5887	0.0192	17.654	0.869	0.2175	0.0072	2962.4	54.2	100.7
8.1	core†	501	51	0.10	308	3	0.02	0.5751	0.0270	17.188	1.256	0.2168	0.0109	2956.9	83.7	99.0
15.2	mantle§	880	63	0.07	535	4	0.02	0.5712	0.0092	17.059	0.281	0.2166	0.0004	2955.7	3.3	98.5
18.2	mantle†	784	56	0.07	481	45	0.20	0.5765	0.0093	17.159	0.293	0.2159	0.0009	2950.2	6.6	99.5
14.1	core ≈	475	109	0.24	287	35	0.27	0.5499	0.0090	16.346	0.276	0.2156	0.0006	2948.0	4.4	95.8
5.1	core§	723	49	0.07	447	2	0.01	0.5828	0.0048	17.288	0.145	0.2152	0.0002	2944.8	1.8	100.5
6.2	rim†	894	19	0.02	481	7	0.03	0.5244	0.0085	13.608	0.226	0.1882	0.0004	2726.5	3.1	99.7
11.1	rim§	1056	31	0.03	574	5	0.02	0.5294	0.0044	13.583	0.119	0.1861	0.0004	2708.0	3.4	101.1
12.1	rim§	1211	36	0.03	645	5	0.02	0.5200	0.0084	13.188	0.217	0.1840	0.0002	2688.9	2.1	100.4
5.2	rim§	935	26	0.03	506	30	0.12	0.5277	0.0085	13.373	0.225	0.1838	0.0006	2687.5	5.0	101.6
13.3	rim§	1487	45	0.03	779	15	0.04	0.5113	0.0083	12.886	0.217	0.1828	0.0005	2678.4	4.6	99.4
13.2	rim§	1550	50	0.03	842	14	0.03	0.5300	0.0085	13.334	0.217	0.1825	0.0002	2675.5	2.1	102.5
16.2	rim§	1169	40	0.04	617	29	0.10	0.5157	0.0085	12.918	0.238	0.1817	0.0012	2668.3	10.9	100.5
10.1	rim§	1434	16	0.01	717	19	0.06	0.4912	0.0114	12.225	0.295	0.1805	0.0008	2657.4	7.5	96.9

Uncertainties reported at 1s and are calculated by numerical propagation of all known sources of error, and data corrected according to procedures outlined in Stern (1997). *=Radiogenic Pb; f206c=percent ^{206}Pb contribution from common Pb; ‡=^{207}Pb/^{206}Pb age. Conc.=concordance=100×(^{206}Pb/^{238}U age)/(^{207}Pb/^{206}Pb age). CL or BSE characteristics: †=Oscillatory-zoned; ¶=straight/parallel zoning; §=unzoned/structureless; ≈=weakly or irregularly zoned.

ite preserve relatively simple growth structures, namely, straight, broad, banded or feathery zoning, characteristic of igneous crystallisation, which constitutes much of the grains. Delicate oscillatory growth, though not readily apparent in CL, is common in some of the more prismatic and elongate prism subpopulations, as evidenced through BSE imaging (not shown). A number of zircon grains have distinct, angular or irregular, zoned cores surrounded by a uniform (unzoned) mantle or overgrowth. In some cases, the initial mantle is a thin, low U (bright CL) domain, succeeded by a broader, higher U exterior (dark CL; e.g. Fig. 5a, grains 4, 3, 20, and 2).

Of the 39 spot analyses, two-thirds have ^{207}Pb/^{206}Pb ages >3600 Ma (Fig. 4a). Very few of these older analyses show any significant evidence of discordance or Pb loss. The oldest ^{207}Pb/^{206}Pb ages were measured from two small, distinct, structural inner cores in grains 14 (3730±4 Ma, 2σ; Fig. 5a) and 22 (3695±6 Ma, 2σ, 5% discordant), interpreted as xenocrystic fragments incorporated in the tonalite magma from older crust. The majority of analyses cluster on or near concordia between ~3650 and 3624 Ma, and 20 of these yield a weighted mean ^{207}Pb/^{206}Pb age of 3640±3 Ma (95% confidence). Because these age domains (i) are characterised by regular, simple magmatic zoning, (ii) comprise most of the zircon volume and (iii) define an apparently single population of ages, we interpret 3640±3 Ma to represent the magmatic crystallisation age of the tonalite protolith. Many of these domains have Th/U ratios that would be considered average for zircons precipitated from a tonalitic magma (e.g. 0.7–1.0; Table 1).

The full spectrum of spot ages from the tonalite mylonite spans more than 1.0 Ga, with several analyses from discrete, cross-cutting overgrowths on older zircon cores yielding ages ranging from 2978 to 2605 Ma (e.g. grains 2, 20, Fig. 5a; Table 1). All of the analysed overgrowths have very low Th/U ratios, between about 0.080 and 0.018, in almost all cases a consequence of low Th contents, and we interpret the overgrowth ages to reflect subsequent metamorphism imposed on the tonalite. Given the limited data we were able to collect on the generally thin zircon

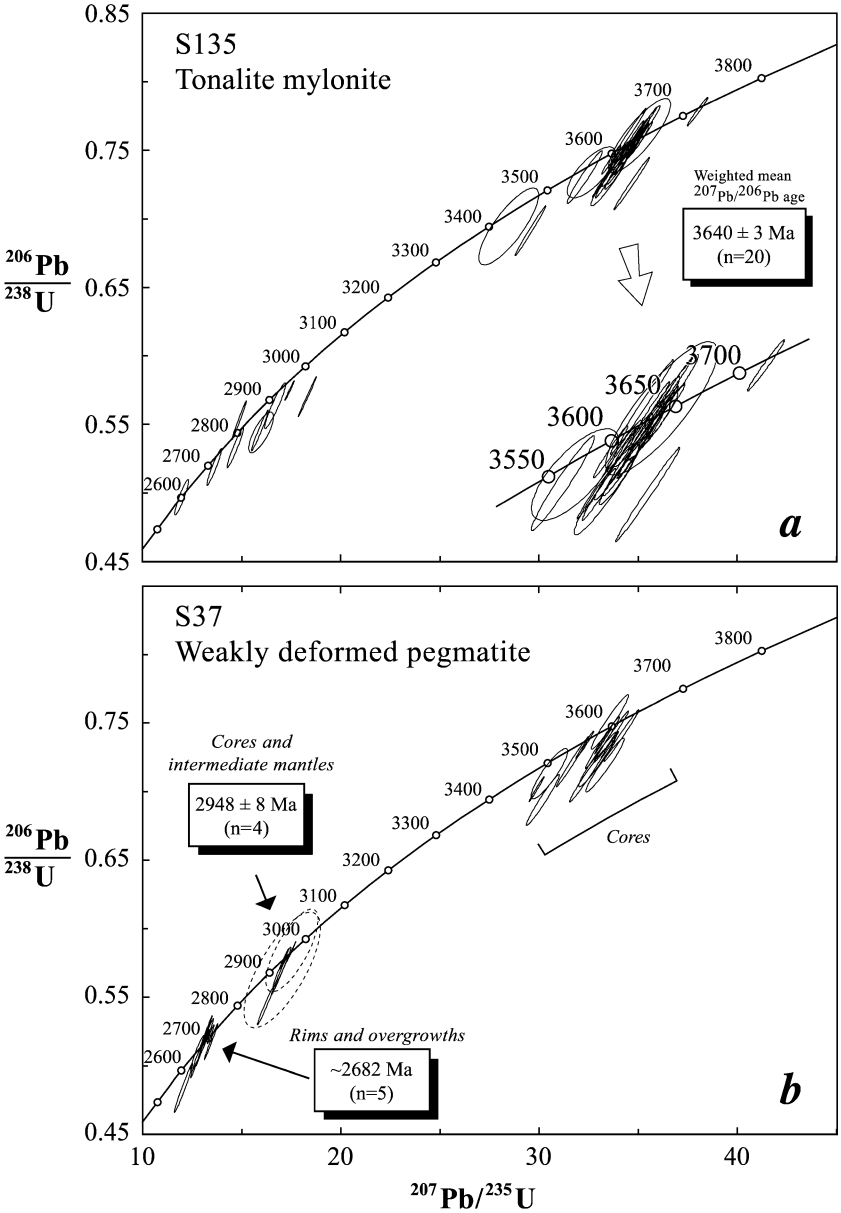

Fig. 4. Concordia diagrams showing SHRIMP U–Th–Pb data for Isua thrust-nappe stack units: (a) tonalite mylonite (S135; with inset of older age population); (b) pegmatite (S37).

rims, a comprehensive understanding of the significance of the younger overprinting event(s) remains elusive. This is complicated by the fact that some of the overgrowth analyses are slightly discordant and because unambiguous modelling of Pb loss in these is not possible. The most precise and oldest overgrowth age obtained was on the thick exterior shell of grain 2 (Fig. 5a) at 2978±3 Ma (2σ; Th/U=0.018). This age and slightly more discordant ages determined on thin overgrowths on grains 17 and 19 (2942±22 and 2926±52 Ma, 2σ, respectively) are discussed later in the light of results from pegmatite S37. Finally, we

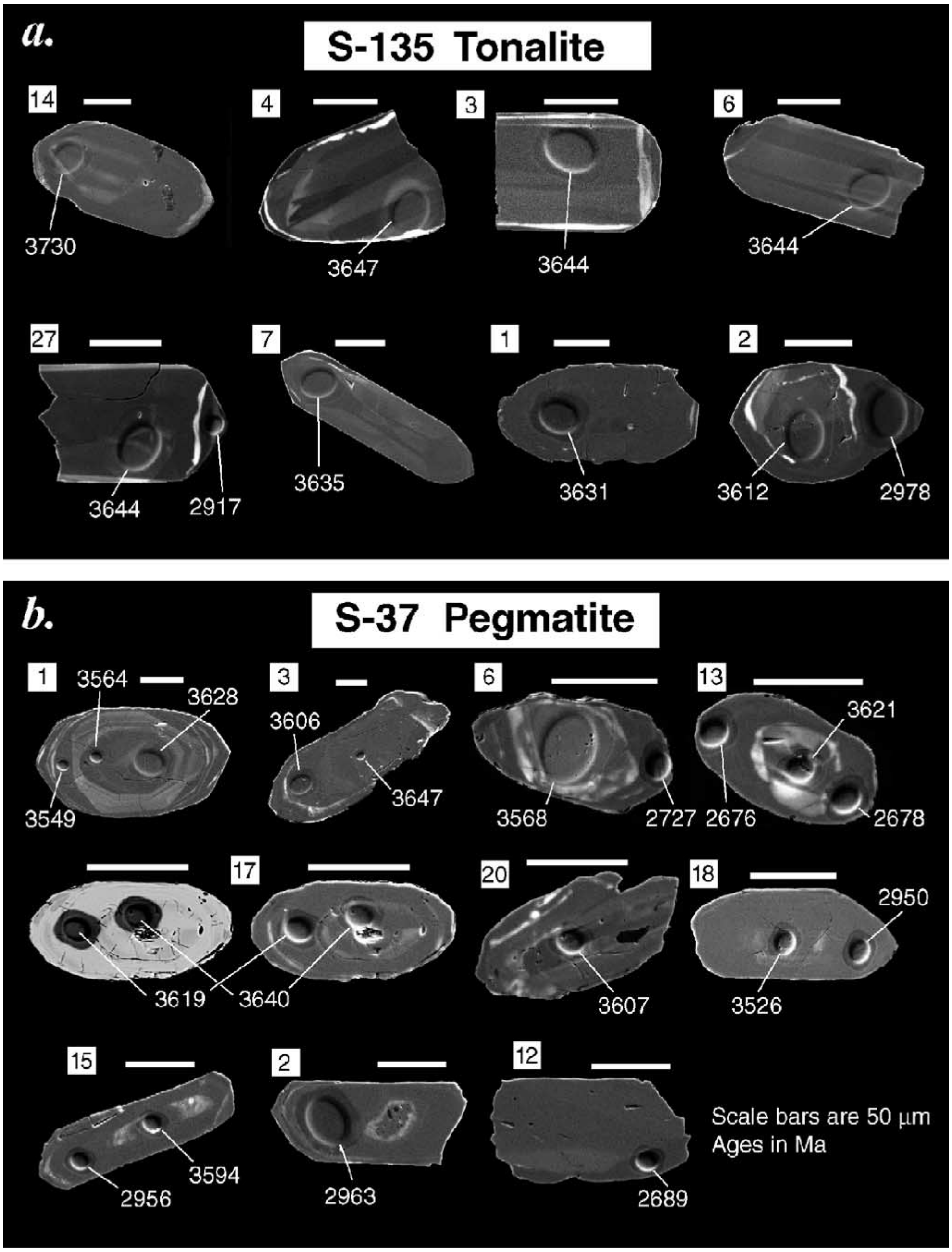

Fig. 5. SEM images of selected zircons, illustrating principal morphological groups and internal growth complexities. Keyed to Table 1, grain identity numbers are shown adjacent each zircon, as are $^{207}Pb/^{206}Pb$ ages (in Ma) corresponding to each ovoidal SHRIMP ablation pit. (a) Cathodoluminescence (CL) images of grains from the tonalite mylonite (S135). (b) CL images of zircons from the pegmatite (S37). Grain 17 features a backscattered electron (left) and CL image (right) pair. Scale bars shown are all 50 μm in length.

interpret the spread in $^{207}Pb/^{206}Pb$ ages for spot analyses of cracked, high U grain centres between 3586 and 3070 Ma as a direct consequence of incomplete Pb loss, either between about 3000 and 2700 Ma, or recently, or both.

4.1.2. Pegmatite, S37

This mildly folded pegmatite yielded abundant zircons of variable quality from which representative non-paramagnetic and paramagnetic fractions at 0° and 1° side slope (maximum current, Frantz) were selected. These comprise a wide diversity of grain types, from colourless to pale yellow, cloudy or turbid subhedra, to pale brown and deeper brown, rounded subhedral grains, as well as subequant or elongate (up to 4:1) varieties. By comparison with S135, the majority of zircons in S37 are slightly smaller. In transmitted light, a high proportion of grains appear heavily cracked and many contain visible cores and overgrowths, while others preserve fine, oscillatory zoning. In some zircons, cores that were not evident in transmitted light were apparent in BSE mode (e.g. grain 20, Fig. 5b).

Representative images of zircons from S37 are shown in Fig. 5b. In contrast to zircons from the tonalite mylonite S135, these grains lack wide, igneous-zoned centres. Rather, the central portions of many zircons are characterised by smaller, angular or irregular cores with chaotic, wispy or mottled CL textures (e.g. Fig. 5b, grains 13, 17, 20, 18, 15), while others have cores charged with numerous inclusions (grain 2), or are relatively large and structureless. However, a small minority of grains show large, oscillatory-zoned interiors (cores?) surrounded by thin rims or overgrowths (e.g. grain 1). Zircon analyses span a wide range of $^{207}Pb/^{206}Pb$ ages, for the most part on or near concordia, between about 3650 and 2650 Ma (Table 1; Fig. 4b). Model $^{207}Pb/^{206}Pb$ ages for the oldest population fall between 3647 and 3516 Ma and characterise cores or inner mantles developed around them. They are more discordant and dispersed than the comparable population recovered from S135. Grains 3 and 17 (Table 1; Fig. 5b) both display weakly zoned or unzoned ~3647–3640 Ma cores, surrounded by younger ~3619–3606 Ma mantles with consistently lower Th/U. In such cases, igneous or metamorphic cores were probably rimmed by new growth or recrystallisation of zircon during a later metamorphic event at ~3619–3606 Ma. Grain 1 shows a similar relationship but may have suffered a greater degree of Pb loss. Note that in all three grains, U content in the rim passes rapidly outward from low (bright CL) to elevated, uniform values toward the grain boundary. In seven grains, ages were measured in either broad, thick, unzoned or oscillatory-zoned "intermediate mantles" surrounding smaller cores (e.g. Fig. 5b, grains 15, 18, and 2), or in equivalent broad centres lacking older cores (e.g. Table 1, grains 5, 7, and 8). These domains have $^{207}Pb/^{206}Pb$ ages which define a very tight cluster between 2963 and 2945 Ma. Although two of the analyses have large analytical errors (7.1 and 8.1, Table 1; dashed ellipses in Fig. 4b), the four youngest and most precise measurements yield a mean age of 2948 ± 8 Ma (2σ). The data presented in Table 1 probably understate the significance and distribution of these ~2950 Ma growth domains because more attention was devoted during analysis to understanding the spectrum of ages represented by the diversity of xenocrystic cores. Some of these grains have elongate and generally prismatic habit (e.g. grains 2, 15, Fig. 5b), alternately displaying delicate oscillatory (i.e. magmatic) zoning or 'flat', unzoned internal structure. Accordingly, we interpret 2948 ± 8 Ma to represent the age of crystallisation of the pegmatite; the core ages imply derivation from an orthogneissic source whose evolution spanned ~3650–3500 Ma. As mentioned above, a subset of the $^{207}Pb/^{206}Pb$ ages determined on zircon rims from the tonalite (S135) falls within the range 2978–2926 Ma (Table 1) and imply that some recrystallisation or complete Pb loss around older zircon cores took place ca. 2950 Ma, synchronous with the emplacement of the pegmatite.

Thin rims, present on most grains in S37, are largely either unzoned or weakly zoned and individually define the youngest cluster of $^{207}Pb/^{206}Pb$ ages, between 2708 and 2657 Ma (Table 1, Fig. 4b). Analysis 6.2 has a slightly older age of 2727 Ma, but post-analysis reimaging suggests that the primary beam in this spot location probably straddled not just the exterior rim, but also an 'intermediate mantle' domain (e.g. 2950 Ma); its mixed age therefore has no geological significance. All of the rim domains are characterised by high U contents and consistent, very low Th/U ratios, between 0.012 and 0.036, and undoubtedly grew during a metamorphic event. We

Table 2
Thermal ionisation mass spectrometry (TIMS) U–Pb analytical data for zircons from Taserssuaq tonalite (D73)

Analysis[a]	Weight[b] (μg)	Concentration[c]			Atomic ratios[d]					Age (Ma)[e]	
		U (ppm)	Pb* (ppm)	Pb_c (pg)	$^{206}Pb/^{204}Pb$	$^{208}Pb/^{206}Pb$	$^{206}Pb/^{238}U$	$^{207}Pb/^{235}U$	$^{207}Pb/^{206}Pb$	$^{207}Pb/^{206}Pb$	Conc.[f] (%)
Taserssuaq tonalite at lat. 65°06′ 57″N, long. 50°17′ 10″W											
Z1 st, pk	14	56	38.7	27	1067	0.144	0.5914±0.16	18.053±0.17	0.22139±0.04	2990.8±1.3	100.1
Z2 st, pk	8	57	39.1	24	685	0.128	0.5913±0.20	18.059±0.20	0.22153±0.06	2991.8±1.7	100.1
Z3 st, pk	6	71	48.9	31	525	0.134	0.5919±0.23	18.044±0.24	0.22109±0.05	2988.7±1.6	100.3
Z4 el, pk	7	75	52.0	26	762	0.139	0.5906±0.15	18.039±0.16	0.22152±0.05	2991.8±1.7	100.0
Z5 el, co	9	27	18.8	25	362	0.151	0.5907±0.31	17.991±0.31	0.22090±0.11	2987.3±3.5	100.2

[a] Grain characteristics (co, colourless; el, elongate; pk, pink; st, stubby).
[b] Weight of grains estimated visually using a microscope.
[c] Concentration uncertainty varies with sample weight: estimated at >10% for sample weights <10 μg, <10% for sample weights >10 μg. Pb*, radiogenic Pb; Pb_c, total common Pb in analysis corrected for spike and fractionation.
[d] Ratios corrected for spike, fractionation, blank, and initial common Pb, except $^{206}Pb/^{204}Pb$ ratio corrected for spike and fractionation only. Errors are 1σ in percent.
[e] Errors are 2σ in Ma.
[f] Concordance=100×($^{206}Pb/^{238}U$ age)/($^{207}Pb/^{206}Pb$ age).

interpret the average age for the rims to be ~2682 Ma, calculated using the most clustered subset. However, there is considerable scatter, and we acknowledge that further work is required to more accurately and precisely define the timing of Neoarchean metamorphism that affected this sample.

4.2. TIMS

4.2.1. Taserssuaq tonalite, D73

Pink to colourless, elongate (aspect ratio of 3:1:1) to stubby (aspect ratio of 5:3:1) prismatic zircon grains were obtained from the Taserssuaq tonalite (D73). The clearest and least magnetic grains with the fewest inclusions and cracks were abraded (Krogh, 1982). U–Pb dating by conventional isotope dilution thermal ionisation mass spectrometry was performed on five single grains. Routine sample preparation and analytical procedures were similar to those described in Dubé et al. (1996). All analyses are concordant with $^{207}Pb/^{206}Pb$ ages of 2992–2987 Ma (Table 2; Fig. 6). The igneous crystallisation age of the tonalite is interpreted as 2991±2 Ma. This is indistinguishable, within error, from the 2982±7 Ma age reported by Garde et al. (1986).

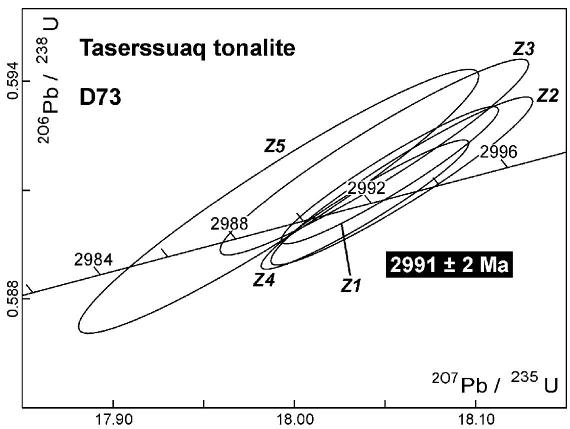

Fig. 6. Concordia diagrams showing TIMS U–Pb data for zircons from the Taserssuaq tonalite (D73).

5. Discussion

5.1. Paleoarchean thrust-nappe tectonics

Extensive, published geochronology acquired over the past 30 years demonstrates that the principal tectonothermal and magmatic events in the Akulleq terrane occurred during two extended periods: ~3870–3500 and ~2840–2700 Ma (e.g. Nutman et al., 1996, 2000; Friend et al., 1996; Frei et al., 1999; Frei and Rosing, 2001 and references therein). In addition, ~2980 Ma regional metamorphism that occurred in the adjacent Akia terrane (Nutman et al., 1989; Garde et al., 2000) is contemporaneous with the emplacement of the Taserssuaq tonalite (D73), and zircon rims and overgrowths dated at ~2950 and ~2680 Ma in both our samples S135 and S37 are broadly comparable to (i) the ~2980 Ma event in the Akia terrane (Nutman et al., 1989) and (ii) the ~2720 Ma granitoid sheets common to the Akulleq, Akia, and Tasiusarsuaq terranes (Friend et al., 1996). Although the Paleoarchean history of the Akulleq terrane is the subject of lively debate (e.g. Kamber and Moorbath, 1998; Whitehouse et al., 1999; Nutman et al., 2000 and references therein), there is general agreement that a major regional tectonothermal event occurred at ~3650 Ma, manifested as the emplacement of tonalite plutons, as well as granulite facies metamorphism in the vicinity of Godthåbsfjord and amphibolite facies metamorphism and the intrusion of granitoid sheets at higher crustal levels in the Isukasia area (e.g. Nutman et al., 1996; Crowley and Myers, 2001). We emphasise that, in the Akulleq terrane as a whole, no regional tectonothermal event has so far been documented in the interval 3500–2840 Ma, and the principal Paleoarchean regional deformation event occurred at ~3650 Ma.

Our results indicate that the deformation history of the mylonitic, crystalline thrust-nappe stack beneath the western limb of the Isua Greenstone Belt occurred prior to emplacement of the 2991±2 Ma Taserssuaq tonalite (D73). It could be argued that the mylonites cut by the Taserssuaq tonalite lie on the Akia side of a Neoarchean terrane boundary, now marked by the Ataneq fault, and are unrelated to those on the Akulleq side. However, field observation demonstrates that the mylonites on either side of the Ataneq fault are part of the same thrust-nappe stack (Hanmer and Greene, 2002). Furthermore, the cross-cutting 2948±8 Ma pegmatite (S37) provides a minimum age for intense deformation of the thrust-nappe stack, compatible with that obtained from the Taserssuaq tonalite. Moreover, we interpret the 3640±3 Ma tonalite mylonite (S135) to be part of the swarm of synkinematic tonalite sheets emplaced during mylonitisation which, if valid, would indicate that shearing in the thrust-nappe stack was active during the Paleoarchean. This interpretation is supported by the presence of the 2991±2 Ma Taserssuaq tonalite and the 2948±8 Ma pegmatite, both of which are post-mylonite, and the known temporal distribution of tectonothermal events in the Akulleq terrane. Accordingly, we propose that the mylonitic crystalline thrust-nappes in the footwall of the western part of the Isua Greenstone Belt formed during the Paleoarchean at ~3640 Ma. Finally, the open folding that affected the 2948±8 Ma pegmatite likely corresponds to mild Neoarchean reactivation of the thrust-nappe stack (see Hanmer and Greene, 2002).

In short, our geochronological results reflect the known temporal distribution of tectonothermal and magmatic events in the Godthåbsfjord region, i.e. ~3650, ~3000, and ~2720 Ma. From this, we conclude that the mylonitic crystalline thrust-nappes in the footwall of the western part of the Isua Greenstone Belt formed during the Paleoarchean (~3640 Ma) and constitute the oldest thrust-nappe stack known on Earth. Furthermore, Hanmer and Greene (2002) contend that the structural regime of the mylonitic thrust-nappe stack is very similar to that of Phanerozoic and modern mountain belts and that the deformational behaviour, rheological constitution, and overall strength of Paleoarchean and modern continental crust were comparable.

5.2. Neoarchean accretionary tectonics?

Our structural (Hanmer and Greene, 2002) and geochronological results lead us to reexamine the Akia–Akulleq interface as an accretionary boundary. In their original model, Friend et al. (1987) identified three terranes, Tasiusarsuaq, Faeringhavn, and Tre Brødre, separated from each other by narrow (~10 m) mylonitic shear zones. The Tre Brødre terrane was distinguished because it contained no Paleoarchean rocks and had never seen granulite facies metamorphism, in contrast to the Faeringhavn terrane. However, as the model evolved, this definition did not prove to be robust, and the Akia terrane was identified, though little emphasis was placed on its definition (Friend et al., 1988). When it was subsequently established that the Tre Brødre and Faeringhavn terranes had much in common with each, they were demoted and amalgamated into the Akulleq terrane (Fig. 1B; McGregor et al., 1991).

At all stages of its formulation, the Neoarchean accretionary model has emphasised the abrupt break at the Akulleq–Tasiusarsuaq boundary interpreted to mark the lower boundary of a tilted crustal section in the hanging wall, with retrogressed granulites at the base passing up structural section into shallower crustal levels. Fluid flux and retrogression of the granulites were attributed to underthrusting of the Akulleq terrane along the Qarliit nunaat thrust (e.g. McGregor et al., 1991). In contrast, the Akia–Akulleq boundary was less rigorously defined. Metamorphic grade in the southeastern part of the Akia terrane and in parts of the Akulleq terrane never exceeded amphibolite facies. Hence, we suggest that the boundary is not an abrupt metamorphic break. Furthermore, the Ivinnguit fault is heavily overprinted and is only preserved undisturbed along relatively short island segments in Godthåbsfjord (e.g. Friend and Nutman, 1991) where it is overturned (e.g. Friend et al., 1988). In light of our geochronological results, it appears that the ~2980 Ma high-grade regional metamorphism that characterises the Akia terrane was recorded in the zircons of the mylonitic footwall to the Isua Greenstone Belt at about the same time as the Akia–Akulleq boundary was stitched by the Taserssuaq tonalite. Accordingly, our combined structural and geochronological results indicate that, if this is an important tectonic boundary, deformation associated with it must have occurred prior to ~3000 Ma, at or before ~3640 Ma, possibly by emplacement of the Akulleq onto the southern part of the Akia terrane. However, geochronological study of the Akia terrane, focused in the central part, has revealed no rocks older than ~3220 Ma (Garde et al., 2000). Moreover, we note that juxtaposition of different geological histories and metamorphic grades across shear zones does not necessarily require the accretion of exotic terranes (e.g. Sengor and Dewey, 1991; Percival and West, 1994; Hanmer et al., 2000). Alternatively, assuming that Neoarchean accretion did indeed occur in the Godthåbsfjord region at ~2820–2720 Ma (Friend et al., 1996; see also Friend and Nutman, 2001; Rosing et al., 2001) and that a terrane boundary separates the central Akia terrane and the Akulleq terrane as suggested by the contrasting Nd isotopic signatures, an accretionary boundary may lie within the currently defined boundaries of the Akia terrane.

6. Conclusions

We interpret new geochronological constraints from a stack of mylonitic, crystalline thrust-nappes, located in the footwall of the western part of the Isua Greenstone Belt, to indicate that the thrust-nappe stack formed during the Paleoarchean at ~3640 Ma, thereby representing the oldest known example on Earth. This structural regime is very similar to that of Phanerozoic and modern mountain belts, suggesting that the deformational behaviour, rheological constitution and overall strength of Paleoarchean and modern continental crust were comparable.

The Paleoarchean thrust-nappe stack lies adjacent to a purported accretionary boundary between Akia and Akulleq terranes that were supposedly juxtaposed during Neoarchean (~2820–2720 Ma) southwest-directed thrusting of the former over the latter. However, the boundary is stitched by the 2991±2 Ma Taserssuaq tonalite, and the thrusting, which we interpret to be Paleoarchean in age, was directed toward the Northwest. We conclude that the Akia–Akulleq boundary in the Isukasia area is a northwest-vergent Paleoarchean structure, rather than a southeast-vergent Neoarchean suture. If a Neoarchean accretionary boundary exists between rocks of the Akia and Akulleq terranes, it has not yet been identified, but it must lie within the Akia terrane, which would thereby require redefinition.

Acknowledgements

Thanks are expressed to the Danish Natural Science Research Council, to the Commission for Scientific Research in Greenland, and to the Minerals Office, Greenland Government, for generous support to the Isua Multidisciplinary Research Project (IMRP) to which this is a contribution. In particular, we are indebted to Peter Appel, Geological Survey of Denmark and Greenland, for his consistent support and encouragement. We thank Richard Stern for reading an early version of the manuscript and Adam Garde and Stephen Moorbath for their thoughtful, critical journal reviews. This is Geological Survey of Canada contribution 2001071.

References

Appel, P.W.U., Fedo, C.M., Moorbath, S., Myers, J.S., 1998. Early Archaean Isua supracrustal belt, West Greenland: pilot study of the Isua multidisciplinary research project. Geology of Greenland Survey Bulletin 180, 94–99.

Appel, P.W.U., Fedo, C.M., Moorbath, S., Myers, J.S., 1998. Recognizable primary volcanic and sedimentary features in a low strain domain of the highly deformed, oldest known (~ 3.7–3.8 Gyr) greenstone belt, Isua, West Greenland. Terra Nova 10, 57–62.

Blichert-Toft, J., Frei, R., 2001. Complex Sm–Nd and Lu–Hf isotope systematics in metamorphic garnets from the Isua supracrustal belt, West Greenland. Geochimica et Cosmochimica Acta 18, 3177–3187.

Boak, J.L., Dymek, R.F., 1982. Metamorphism of the ca. 3800 Ma supracrustal rocks at Isua, West Greenland: implications for early Archaean crustal evolution. Earth and Planetary Science Letters 59, 155–176.

Chadwick, B., Crewe, M.A., Park, J.F.W., 1983. Field work in the north of the Ivisârtoq region, inner Godthåbsfjord, southern West Greenland. Rapport—Grønlands Geologiske Undersøgelse 115, 49–56.

Crowley, J.L., Myers, J.S., 2001. Early Archean tectonic history of 3820–3640 Ma granitoid rocks adjacent to the Isua greenstone belt, southern West Greenland. 4th International Archean Symposium, Perth, Australia, Programme with Abstracts, vol. 4, pp. 297–298.

de Wit, M.J., 1998. On Archean granites, greenstones, cratons and tectonics: does the evidence demand a verdict? Precambrian Research 91, 181–226.

Dubé, B., Dunning, G.R., Lauzière, K., Roddick, J.C., 1996. New insights into the Appalachian orogen from geology and geochronology along the Cape Ray fault zone, southwest Newfoundland. Bulletin of the Seismological Society of America 108, 101–116.

Frei, R., Rosing, M., 2001. The least radiogenic terrestrial leads; implications for the early Archean crustal evolution and hydrothermal–metasomatic processes in the Isua Supracrustal Belt (West Greenland). Chemical Geology 181, 47–66.

Frei, R., Bridgwater, D., Rosing, M., Stecher, O., 1999. Controversial Pb–Pb and Sm–Nd isotope results in the early Archean Isua (West Greenland) oxide iron formation: preservation of primary signatures versus secondary disturbances. Geochimica et Cosmochimica Acta 63, 473–488.

Friend, C.R.L., Nutman, A.P., 1991. Refolded nappes formed during late Archaean terrane assembly, Gothåbsfjord, southern West Greenland. Journal of the Geological Society 148, 507–519.

Friend, C.R.L., Nutman, A.P., McGregor, V.R., 1987. Late-Archaean tectonics in the Faeringhavn-Tre Brødre area, south of Buksefjordeen, southern West Greenland. Journal of the Geological Society 144, 369–376.

Friend, C.R.L., Nutman, A.P., 2001. U–Pb zircon study of tectonically bounded blocks of 2940–2840 Ma crust with different metamorphic histories, Paamiut region, South-West Greenland: implications for the tectonic assembly of the North Atlantic craton. Precambrian Research 105, 143–164.

Friend, C.R.L., Nutman, A.P., McGregor, V.R., 1988. Late Archaean terrane accretion in the Godthab region, southern West Greenland. Nature 355, 535–538.

Friend, C.R.L., Nutman, A.P., Baadsgaard, H., Kinny, P.D., McGregor, V.R., 1996. Timing of late Archean assembly, crustal thickening and granite emplacement in the Nuuk region, southern West Greenland. Earth and Planetary Science Letters 142, 353–365.

Garde, A.A., 1987. Geological map of Greenland, 1:100 000, Isukasia 65 V.2 Syd, scale 1:100 000.

Garde, A.A., 1997. Accretion and evolution of an Archaean high-grade grey gneiss–amphibolite complex: the Fiskefjord area, southern West Greenland. Geology of Greenland Survey Bulletin 177, 115.

Garde, A.A., Larsen, O., Nutman, A.P., 1986. Dating of late Archean crustal mobilisation north of Qugssuk, Godthåbsfjord, southern West Greenland. Rapport—Grønlands Geologiske Undersøgelse 128, 23–36.

Garde, A.A., Friend, C.R.L., Nutman, A.P., Marker, M., 2000. Rapid maturation and stabilisation of middle Archaean continental crust: the Akia terrane, southern West Greenland. Bulletin of the Geological Society of Denmark 47, 1–27.

Hamilton, W.B., 1998. Archean magmatism and deformation were not products of plate tectonics. Precambrian Research 91, 143–179.

Hanmer, S., Greene, D.C., 2002. A modern structural regime in the early Archean (~ 3.64 Ga); Isua Greenstone Belt, southern West Greenland. Tectonophysics 346, 201–222.

Hanmer, S., Corrigan, D., Pehrsson, S., Nadeau, L., 2000. SW Grenville Province, Canada: the case against post-1.4 Ga accretionary tectonics. Tectonophysics 319, 33–51.

Hayashi, M., Komiya, T., Nakamura, Y., Maruyama, S., 2000. Archean regional metamorphism of the Isua supracrustal belt, southern West Greenland: implications for a driving force for Archean plate tectonics. International Geology Review 42, 1055–1115.

James, P.R., 1976. Deformation of the Isua block, West Greenland: a remnant of the earliest stable continental crust. Canadian Journal of Earth Sciences 13, 816–823.

Kamber, B.S., Moorbath, S., 1998. Initial Pb of the Amîtsoq gneiss revisited: implication for the timing of early Archaean crustal evolution in West Greenland. Chemical Geology 150, 19–41.

Krogh, T.E., 1982. Improved accuracy of U–Pb zircon ages by the creation of more concordant systems using an air abrasion technique. Geochimica et Cosmochimica Acta 46, 637–649.

McGregor, V.R., Friend, C.R.L., Nutman, A.P., 1991. The late Archaean mobile belt through Godthabsfjord, southern West Greenland: a continent–continent collision zone? Bulletin of the Geological Society of Denmark 39, 179–197.

Moorbath, S., O'Nions, R.K., Pankhurst, R.J., 1973. Early Archaean age for the Isua Iron Formation, West Greenland. Nature 245, 138–139.

Myers, J.S., 2001a. Earth's oldest known volcanic and sedimentary rocks: origin and tectonic evolution of the >3.8–3.7 Ga Isua Greenstone Belt, southwest Greenland. 4th International Archean Symposium, Perth, Australia, Programme with Abstracts, vol. 4, p. 67.

Myers, J.S., 2001b. Protoliths of the 3.8–3.7 Ga Isua Greenstone Belt, West Greenland. Precambrian Research 105, 129–141.

Nutman, A.P., 1984. Early Archaean crustal evolution of the Isukasia area, southern West Greenland. In: Kroner, A., Greiling, R. (Eds.), Precambrian Tectonics Illustrated. E. Schweitz. Verlags, Stuttgart, pp. 79–93.

Nutman, A.P., 1986. The early Archaean to Proterozoic history of the Isukasia area, southern West Greenland. Bulletin—Grønlands Geologiske Undersøgelse 154, 80.

Nutman, A.P., Friend, C.R.L., Baadsgaard, H., McGregor, V.C., 1989. Evolution and assembly of Archean gneiss terranes in the Godthabsfjord region, southern West Greenland: structural, metamorphic and isotopic evidence. Tectonics 8, 573–589.

Nutman, A.P., Friend, C.R.L., Kinny, P.D., McGregor, V.R., 1993. Anatomy of an Early Archean gneiss complex: 3900–3600 crustal evolution in southern West Greenland. Geology 21, 415–418.

Nutman, A.P., McGregor, V.R., Friend, C.R.L., Bennett, V.C., Kinny, P.D., 1996. The Itsaq Gneiss Complex of southern West Greenland; the world's most extensive record of early crustal evolution (3900–3600 Ma). Precambrian Research 78, 1–39.

Nutman, A.P., Bennett, V.C., Friend, C.R.L., Rosing, M.T., 1997. ~3710 and ≥3790 Ma volcanic sequences in the Isua (Greenland) supracrustal belt; structural and Nd isotope implications. Chemical Geology 141, 271–287.

Nutman, A.P., Bennett, V.C., Friend, C.R.L., Norman, M.D., 1999. Meta-igneous (non-gneissic) tonalites and quartz-diorites from an extensive ca. 3800 Ma terrain south of the Isua supracrustal belt, southern West Greenland: constraints on early crust formation. Contributions to Mineralogy and Petrology 137, 364–388.

Nutman, A.P., Bennett, V.C., Friend, C.R.L., McGregor, V.R., 2000. The early Archaean Itsaq Gneiss Complex of southern West Greenland: the importance of field observations in interpreting age and isotopic constraints for early terrestrial evolution. Geochimica et Cosmochimica Acta 64, 3035–3060.

Nutman, A.P., Friend, C.R.L., Bennett, V.C., 2001a. 3.5 Ga mafic intrusions, Itsaq Gneiss Complex, Greenland: crustal underplating and extension. 4th International Archean Symposium, Perth, Australia, Programme with Abstracts, vol. 4, p. 71.

Nutman, A.P., Friend, C.R.L., Bennett, V.C., 2001b. Multiple generations of 3.6–3.85 Ga supracrustal rocks, Itsaq Gneiss Complex, Greenland. 4th International Archean Symposium, Perth, Australia, Programme with Abstracts, vol. 4, p. 70.

Okulitch, A.V., 1999. Geological Time Chart, National Earth Science Series Geological Atlas, Geological Survey of Canada Open File 3040.

Percival, J.A., West, G.F., 1994. The Kapuskasing uplift: a geological and geophysical synthesis. Canadian Journal of Earth Sciences 31, 1256–1286.

Rollinson, H.R., 2000. Zoned pelitic garnets record contrasting metamorphic histories from within the 3.8 Ga Isua Greenstone Belt. Eos Transactions American Geophysical Union, Fall Meeting Supplement, 81: V51D-04.

Rosing, M.T., Nutman, A.P., Lofqvist, L., 2001. A new fragment of the early earth crust: the Aasivik terrane of West Greenland. Precambrian Research 105, 115–128.

Sengor, A.M.C., Dewey, J.F., 1991. Terranology: vice or virtue? In: Dewey, J.F., Gass, I.G., Curry, G.B., Harris, N.B.W., Sengor, A.M.C. (Eds.), Allochthonous Terranes, Cambridge Univ. Press, Cambridge, pp. 1–21.

Smith, G.M., Dymek, R.F., 1983. A description and interpretation of the Proterozoic Kobbefjord fault zone, Godthab district, West Greenland. Rapport—Grønlands Geologiske Undersøgelse 112, 113–127.

Stern, R.A., 1997. The GSC sensitive high resolution ion microprobe (SHRIMP): analytical techniques of zircon U–Th–Pb age determinations and performance evaluation. Radiogenic age and isotopic studies: Report 10, Geological Survey of Canada Paper, 1997-F: 1–31.

White, R.V., Crowley, J.L., Parrish, R., David, K., 2000. Gate-crashing the billionth birthday party: intrusion of dyke swarms in the Isua region. Eos Transactions American Geophysical Union, Fall Meeting Supplement, 81: V51D-05.

Whitehouse, M.J., Kamber, B.S., Moorbath, S., 1999. Age significance of U–Th–Pb zircon data from early Archaean rocks of west Greenland—a reassessment based on combined ion-microscope and imaging studies. Chemical Geology 160, 201–224.